Laser propagation and energy absorption by an argon spark

C. V. Bindhu, S. S. Harilal,[a] M. S. Tillack, F. Najmabadi, and A. C. Gaeris
Center for Energy Research, University of California San Diego, 9500 Gilman Drive, La Jolla, California 92093-0438

(Received 13 June 2003; accepted 21 September 2003)

The laser propagation and energy absorption of an argon spark induced by a laser at different pressures is investigated. 8 ns pulses from a frequency-doubled *Q*-switched Nd:YAG laser are used to create the spark. The pressure of the argon is varied from 1 atm to 10 Torr. Significant energy absorption by the plasma is observed at high pressures (>100 Torr) while there is negligible absorption when the pressure is lower than 50 Torr. The plasma kernel showed distinct behavior with respect to laser energy. At a laser energy well above the breakdown threshold, the spark moved only in the backward direction and the forward component was absent indicating the strong absorption of the laser by the spark front. A spiky behavior is observed in the transmitted temporal profiles of the laser at higher energies and at high pressures and can be due to the formation of a self-regulating regime. © *2003 American Institute of Physics.* [DOI: 10.1063/1.1625413]

I. INTRODUCTION

The interest in gas breakdown with laser radiation is the result of a number of potential applications for high-temperature and high-density plasmas. Gas breakdown studies represent the initial step in research in inertial confinement fusion and plasma heating by laser radiation. The initial plasma of a laser-produced breakdown is similar to that of an electric spark discharge, but there are several important differences. For example laser-produced sparks are generally smaller in volume, transient in nature, and possess a different spatial geometry. Moreover, the laser created breakdown is affected by different experimental parameters like laser mode structure variation, optical aberration in the focusing of the laser beam, etc. Laser-induced sparks have been used both as a source for producing x rays[1] and extreme UV radiation[2] in rare gases and to produce ultrafast shutters.[3,4] They are also capable of igniting gaseous mixtures[5] or even extinguishing a diffusion flame.[6]

It is well recognized that for the creation of a laser spark, various mechanisms may act simultaneously and their relative contributions not only depend on initial conditions but also change during the growth of the spark with time. The most important processes involving the creation of a laser-produced spark are multiphoton ionization and cascade ionization. The first process involves the simultaneous absorption of the number of photons required to equal to the ionization potential of a gas. It has been proven that the threshold flux for multiphoton ionization varies with $P^{-1/k}$, where P is the pressure of the gas and k is the number of photons simultaneously absorbed. The cascade process is the absorption of the radiation by free electrons upon collision with atoms or ions until sufficient energy is gained to ionize an atom by an inelastic electron–atom collision. Both of these phenomena are treated theoretically by different groups.[7,8] In intense light, an electron can gain sufficient energy by absorbing photons from the radiation field in collision with neutral atoms to produce ionization. The multiphoton ionization process can generate the initial electrons from which an electron cascade can develop, if the laser irradiance is high enough. Breakdown will occur if the electron density can reach a critical value despite losses due to diffusion, electron attachment, etc., within the duration of the laser pulse. A more detailed calculation of the breakdown threshold was done by Kroll and Watson,[8] in which they review existing literature on various loss processes of importance for breakdown, such as diffusion, attachment, and vibrational and electronic excitation. The breakdown threshold for argon at different pressures are documented by several authors.[9–12] The breakdown threshold increases with decreasing gas pressure and has a P^{-n} dependence which is characteristic of inverse bremsstrahlung absorption. It is reported that the degree by which the threshold depends on pressure was found to be stronger at a shorter wavelength.[13]

Most of the experiments related to laser-induced gas breakdown studies have centered largely on the measurements of breakdown threshold, while little effort has been devoted to the study of energy absorption and propagation in a spark. The present investigation is designed to study the interaction of a focused laser pulse with argon and subsequent energy propagation through the spark medium. The pressure of the argon is varied from 1 atm (760 Torr) to 10 Torr. We have analyzed how much energy can be propagated through a spark medium and how it affects the temporal profiles of the laser. The optical breakdown is created by focusing 532 nm 8 ns pulses from a frequency-doubled *Q*-switched Nd:YAG laser. Fast photography is undertaken to investigate the spatial behavior of the plasma kernel with time. We also examined the temporal profiles of the transmitted laser pulse through the focal volume at different argon pressures.

[a]Electronic mail: harilal@fusion.ucsd.edu

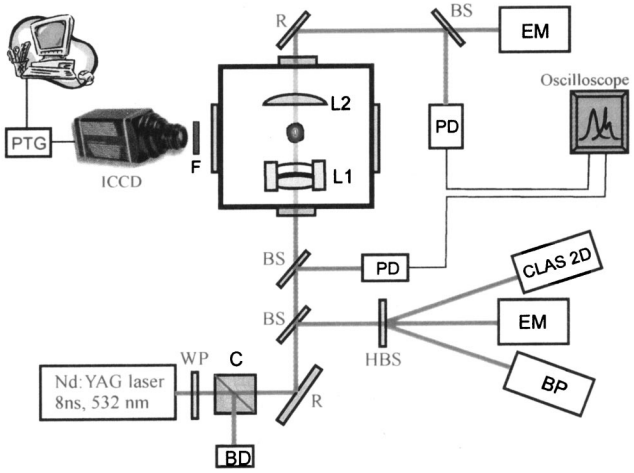

FIG. 1. The schematic of the experimental setup used for imaging, propagation, and energy absorption studies. (F, 532 nm filter; ICCD, intensified charged coupled device; PTG, programmable timing generator; WP, wave plate; C, cube beam splitter; BD beam dump; R, reflector; BS, beam sampler; L1, high-energy laser aplanat; L2, lens; HBS, holographic beam sampler; EM, energy meter; BP, beam profiler; CLAS2D Shack Hartman sensor; and PD, photodiode).

II. EXPERIMENTAL SETUP

The experimental arrangement used for the creation of a laser spark and propagation studies is shown in Fig. 1. We used pulses from a frequency-doubled *Q*-switched Nd:YAG laser [full width at half maximum (FWHM) 8 ns, maximum energy 500 mJ, 10 Hz] for creating breakdown plasma. The pulses were temporally cleaned up by the Quanta Ray injection seeder attachment. The laser pulse parameters were monitored using a photodiode, a beam profiler (Photon Inc.), and a CLAS two-dimensional (2D) wave front sensor (Wavefront Sciences). The spatial structure of the laser profile was approximately Gaussian. The energy of the pulse was varied by using a combination of a wave plate and a cube beam splitter. To create breakdown plasma, the laser pulses were focused using an $f/5$ antireflection coated laser aplanat (CVI Laser, LAP 75.0–15.0) having a focal length of 75 mm. A 75 mm antireflection-coated plano-convex lens is used for collimating the laser beam after passing through the focal region. The optical elements are placed in a vacuum chamber and filled with argon gas.

The kernel imaging was accomplished using an intensified charged coupled device (ICCD, PI MAX, Model 512 RB) placed orthogonal to the laser propagation direction. A Nikon lens was used to image the plume region onto the camera to form a 2D image of the plume intensity. The visible radiation from the plasma was recorded integrally in the wavelength range of 350–900 nm. In order to eliminate 532 nm stray photons from reaching the camera, a magenta subtractive filter was used. A programmable timing generator was used to control the delay time between the laser pulse and the imaging system with an overall temporal resolution of 1 ns.

For propagation studies, photodiodes (Electro-optics Technology, Model EOT 2000, rise time 200 ps) and energy/power meters (Ophir) were used to record temporal profiles and energy of each incoming and transmitted laser pulses through the focal volume. The temporal profiles were monitored using a 1 GHz Digital Phosphor Oscilloscope (Tektronix TDS5014, 5 GS/s maximum real-time sample rate).

III. RESULTS AND DISCUSSION

When a lens focuses the laser beam, the distribution of irradiance in the focal spot is determined by the mode structure in the laser oscillator, by the effect of amplifiers and apertures in the system, and by the parameters of the lens. In the present case, the laser pulses used have a clean temporal profile and have a cross section that is approximately Gaussian. Single element lenses were used in most of the previous experiments[10,14] for focusing a high-power laser beam and a significant spherical aberration was often present, though it may be minimized by the suitable choice of curvatures. The presence of aberrations can lead to erroneous values of optical breakdown threshold even when the measured spot size is used for the determination.[15] The effect of spherical aberration on the distribution of irradiance in the focal region has been calculated by Evans and Morgan.[16] In order to avoid or minimize spherical aberration, we used a two-element laser aplanat for focusing the laser beam. As a rule of thumb, a lens should be considered perfect or diffraction limited, if the optical path difference (OPD) is less than a quarter wave. The estimated OPD of the laser aplanat used in the present studies using Zemax image analysis[17] is about one-fifth of a wave, so the aberration effects are expected to be insignificant.

A. Spatial and temporal evolution of argon spark

Initially, we investigated the kernel behavior at different ambient argon pressures and intensity using 2 ns gated fast photography. Fast photography provides information on spatial and temporal behavior of plasma after the onset of the spark and it is considered to be one of the best diagnostic tools for studying plasma expansion dynamics.[18] The images are taken using the ICCD that views the plasma orthogonal to the laser propagation direction. The shape of the breakdown kernel observed shows interesting behavior. Figure 2 gives the time evolution of argon spark recorded at 1 atm at three different laser energy levels viz. 12 mJ, 55 mJ, and 155 mJ. The duration of the intensification (exposure time) is 2 ns and each image in Fig. 2 is recorded from an independent breakdown event. Timing jitter is less than 1 ns. The laser beam is incident from the left-hand side. For better clarity, all of the images are normalized to their own maximum intensity. This gives a fast on-scale overview of the data.

Once the breakdown occurs and the spark has been formed, it emits radiation whose spectral distribution depends on the temperature.[19–21] At low-energy levels, the plume is confined very close to the focal volume. The shapes of the spark at early times and at low energies are spherical. But as time elapses, the spherical shape is changed to an elliptical shape. With increasing laser energy [Fig. 2(b)], the kernel becomes more asymmetrical in shape; the backward moving plasma (toward the focusing lens) grows much faster than the forward moving plasma (away from the focusing lens). The initiation time is earlier and the rate of growth is

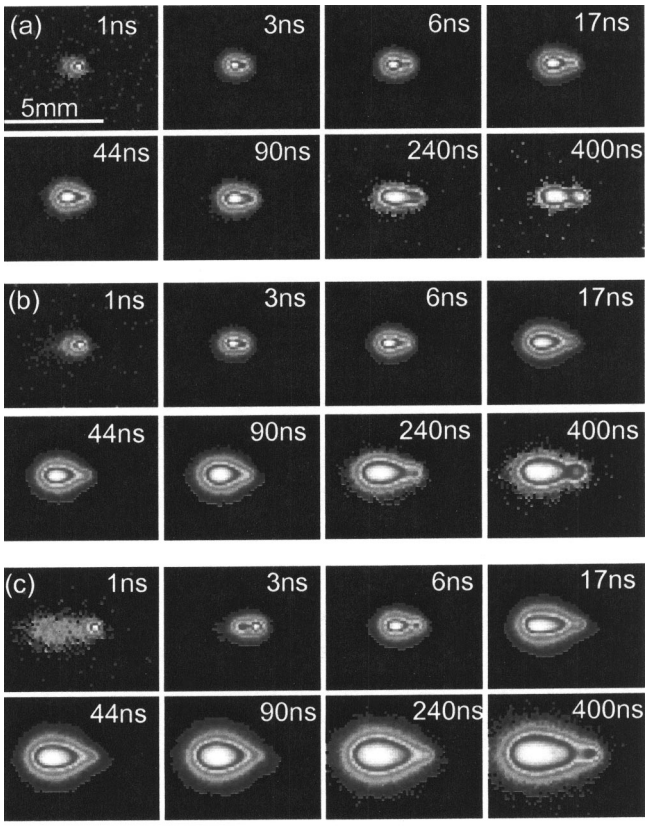

FIG. 2. The time evolution of visible emission from argon spark at 1 atm for different laser energies recorded using an ICCD camera. The exposure time used was 2 ns. The timings in the images represent the time after the onset of plasma formation. All of the images are normalized to their own maximum intensity. The laser is coming from the left-hand side: (a) 12 mJ, (b) 55 mJ, and (c), 155 mJ.

faster if the pulse energy is increased. As we increase the laser energy further [Fig. 2(c)], the forward moving spark component is almost absent. After the initial breakdown, the plasma is heated to a point where it is opaque to the incoming laser beam. The optically thick plasma absorbs practically all of the incident radiation after breakdown.

At higher energies, we observed only the backward moving component of the argon spark. Just after the breakdown event, the layer of gas outside the plasma, although it is transparent to the laser beam, is heated by the plasma radiation. This outside gas close to the plasma will in turn get ionized to such an extent that it will strongly absorb the laser light.[22] This layer will then be further heated very rapidly and the temperature increases. By this time, another layer of plasma nearer the laser will have become strongly absorbing, so the boundary of the plasma will move toward the focusing lens. The absorption of the laser photons by the plasma is mainly due to the inverse bremsstrahlung process, which is so dominant that it leads to the development of a laser supported radiation wave that propagates toward the laser beam. The time scale of this event is that of the laser pulse itself. A simple model for the conditions of a laser-supported radiation wave has been described by Bergel'son *et al.*[23] After the pulse has ended, the plasma will continue to expand, though very slowly. The time evolution of the spark at later times showed dissipation times of ~ 5 ms.[21] It is also noticed that

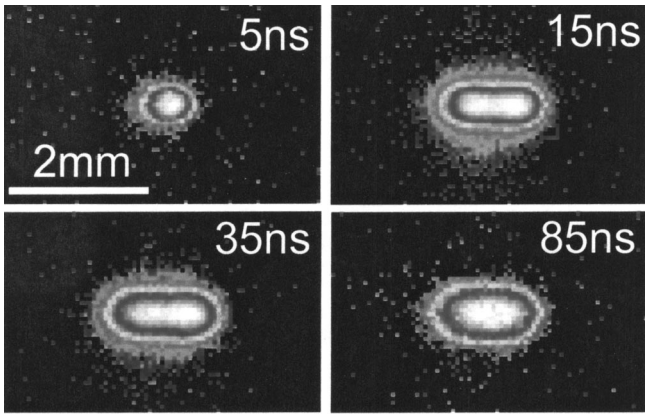

FIG. 3. The time evolution of argon spark images recorded at 50 Torr. The experimental details are same as given in Fig. 2. The laser energy used is 400 mJ.

the shape of the sparks change significantly at later times.[21,24]

The spark emission at low pressures (<100 Torr) has a nearly cylindrical shape. A typical time evolution of an argon spark at 50 Torr is given in Fig. 3. At low pressures, the spark is confined to the focal volume and there is less sign of an absorption front propagating toward the focusing lens. This indicates that multiphoton ionization is dominant at low pressures.

B. Propagation and energy absorption

Our fast photographic studies showed that the argon spark absorption properties depend on laser energy and pressure. In this section, the attenuation of the laser beam passing through the focal spot after breakdown is discussed. Figure 4 gives the experimental results of incident laser energies and the corresponding transmitted laser energies at different argon pressures. At pressures $\geqslant 200$ Torr, significant energy absorption takes place just above breakdown threshold. When breakdown occurs in a dense gas, the attenuation of laser light passing through the focal volume increases abruptly which implies that, following the initiation of breakdown, the free electrons grow to a highly absorbent density within a short period of time. For stronger laser excitation, the electron growth rate is expected to be much faster than the reciprocal of the laser pulse width.[25] Following the rapid growth of electron density, the initial plasma becomes optically thick and absorbs a large fraction of incident energy in the latter portion of the laser pulse. Since significant scattering and diffracted light were not observed in the experiment, the absorbed energies for the breakdown are estimated to be equal to the difference in the incident and transmitted energies.

At 760 Torr argon pressure, the spark absorbs more than 50% of the incident energy just after the breakdown event. As the laser energy increases well above the breakdown threshold, most of the energy ($>80\%$) is absorbed by the spark and a small fraction is transmitted. At still higher energies, the transmitted energy starts to increase gradually with respect to incident energy (see Fig. 4). Figure 5 shows the percentage of absorption varying with argon pressure at

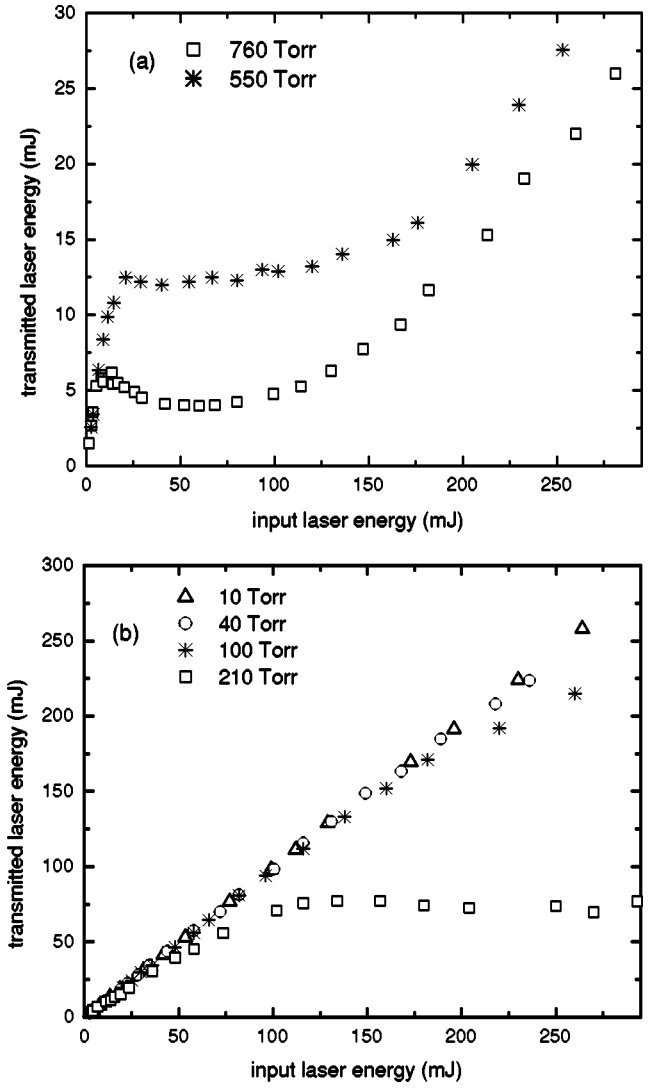

FIG. 4. Variation of transmitted laser energy through the focal volume with input laser energy for different argon pressures: (a) 760 and 550 Torr; and (b) 210, 100, 40, and 10 Torr.

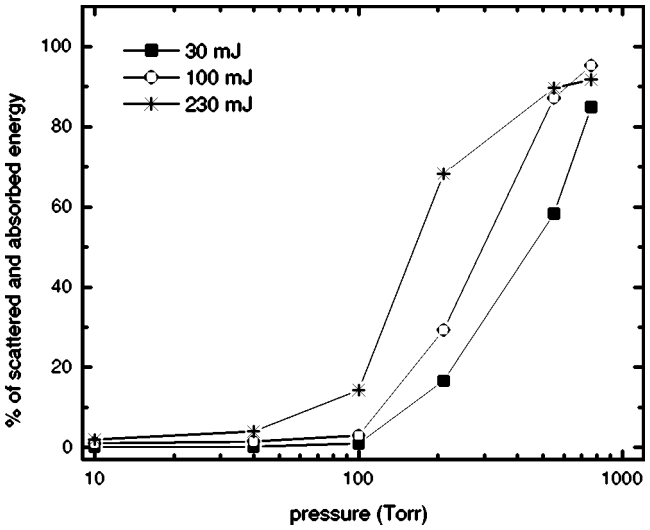

FIG. 5. Percentage of absorbed and scattered energy with different pressures of argon and at different input laser energies.

different incident laser energy levels. The present measurements indicate that when pressure is below 50 Torr, all of the incoming radiation is virtually transmitted through the focal volume without much attenuation. At lower pressures, even after the breakdown event, the spark is found to be less absorptive and most of the energy gets transmitted. At lower pressures, as discussed in the imaging section, the cascade-like growth of the spark is absent and the plasma is confined to the focal volume itself. So a very small fraction of the laser energy is utilized for creating the breakdown event. This spark is less absorptive because the plasma volume is very small compared to high-pressure sparks.

At higher pressures, especially at 760 Torr and 550 Torr, an enhancement in the transmitted signal is observed at higher laser energies. This is expected to be caused by the saturation of plasma absorption. The saturation of laser-produced plasma parameters has been observed and reported in the measurements of the number density of free electrons, electron temperature, etc.[26] When more energy is deposited into the plasma, the induced plasma tends to expand its size instead of becoming hotter and denser.

In order to have a better understanding of the laser absorption by the spark, we examined the temporal profiles of the laser after transmission through the focal volume. Figure 6 gives the normalized temporal profiles of the laser pulse at different laser energies after the laser pulse propagated through the argon spark at different pressure levels of argon. The transmitted temporal profiles are strongly affected by the pressure of the argon gas. At low energies, before the onset of plasma formation, no change in the temporal profile is observed. But, as energy increases, the temporal shape of the transmitted laser pulse changes dramatically. Since the energy absorption process begins only when the laser energy exceeds the breakdown threshold value, the leading edge of the pulse below the threshold is transmitted unperturbed into and through the focal region. Significant perturbation in the transmitted temporal profiles of the laser is observed only at high pressures. At low pressures, especially below 100 Torr, a negligible change in the temporal pattern is observed even if gas breakdown occurs [Fig. 6(c)]. This is supported by the fact that there is a negligible absorption of the laser photons by the plasma at low pressures.

At 760 Torr argon pressure, even at low energies, the argon spark absorbs almost all of the energy after the breakdown event and the transmitted pulse is shortened to 2 ns (FWHM). With increasing energy, the breakdown starts earlier and the transmitted pulse becomes more and more narrow. At still higher energies, as shown in Fig. 6(a), the spark begins to transmit a part of the trailing edge. A spiky behavior in the temporal profiles of the transmitted pulse is observed. We observed this spiky nature in the temporal profiles of a transmitted pulse at high-pressure levels only.

The plot of transmitted laser energy with respect to incident laser energy [Fig. 4(a)] also shows an increase in transmittance at higher energies for argon sparks at high pressures. Mainly, two mechanisms can contribute to the increased transmittance of laser energy at high input energy

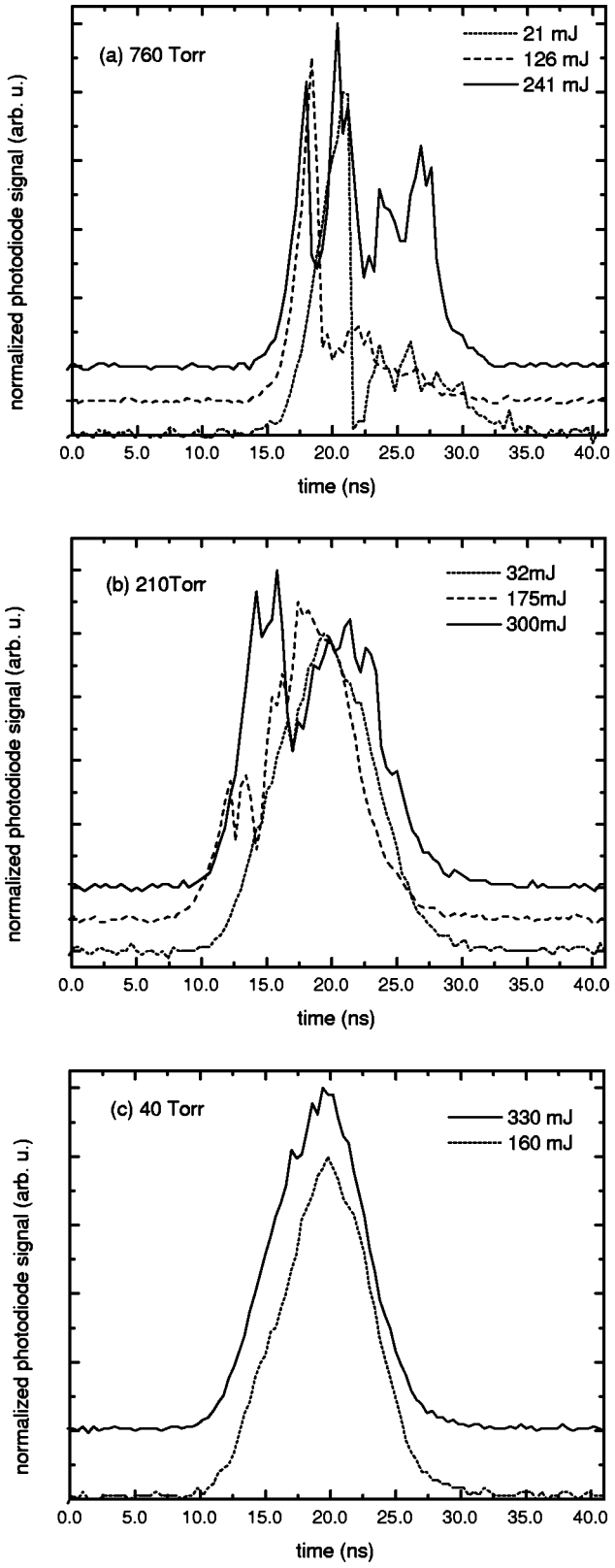

FIG. 6. The temporal structure of the transmitted laser pulse through argon spark at different pressures and for various input laser energies. In each plot, the baseline of all but the lowest energy is offset to be shown on a single plot: (a) −760, (b) −210, and (c) −40 Torr.

levels—self-focusing and absorption saturation. Strong electromagnetic radiation applied to a spark causes the redistribution of electrons and ions. This electron motion continues until the gas dynamic pressure balances the forces exerted on the plasma by the laser field. This leads to a decrease of the electron concentration and hence increases of refractive index on the beam axis, which may lead to self-focusing. But, self-focusing is not evident with 2 ns gated images of sparks. Another plausible mechanism is absorption saturation at higher energies. At high-energy levels, when the spark absorbs an appreciable amount of energy, a self-regulating regime may form. If the absorption of the laser photons by the spark saturates, then the laser photons get transmitted through the spark. But with time, as the spark expands, the density and temperature decrease. This consequently increases the absorption of the laser photons by the spark, which in turn decreases the transmitted photons. This process continues until the end of the laser pulse. This may be the reason for the observed spiky behavior in the transmitted temporal profiles. Similar self-regulating properties have been observed and reported for laser produced plasmas from solid targets.[26,27]

IV. CONCLUSIONS

The laser propagation and energy absorption in argon sparks at pressures ranging from 1 atm to 10 Torr have been investigated. The laser-induced spark is created by focusing 8 ns pulses from a frequency-doubled Nd:YAG laser. The spatial and temporal behavior of laser sparks are investigated using 2 ns fast photography. Spark imaging studies showed that at high pressures the cascade-like process is dominant, while at lower pressures the spark is confined to the focal volume indicating that multiphoton ionization is the dominant mechanism for its creation.

The laser propagation and energy absorption studies showed that at high pressures, spark absorption starts immediately after breakdown and more than 50% of the laser energy is absorbed just above the optical breakdown. At higher pressures, the breakdown threshold represents the highest intensity that can be propagated through a gaseous environment without attenuation. The significant energy absorption by the plasma above the breakdown threshold indicates that inverse bremsstrahlung is important in the subsequent heating and ionization of the plasma. At low pressures, the temporal images of the spark are cylindrical in shape and no backward movement is observed. The spark absorbs a little radiation at low pressure levels for optical breakdown and the attenuation of the beam is negligible.

At high pressures and at high energies, the transmitted energy increased with incident energy and showed spiking behavior in the transmitted pulse. The increased transmittance at higher energies may be caused by absorption saturation. The spiky behavior in the transmitted temporal profiles at higher energies is explained by the formation of a self-regulating regime. At low argon pressures, the transmitted temporal profiles showed negligible changes in their time histories.

[1] X. F. Wang, R. Fedosejevs, and G. D. Tsakiris, Opt. Commun. **146**, 363 (1998).
[2] S. Kranzusch, C. Peth, and K. Mann, Rev. Sci. Instrum. **74**, 969 (2003).

[3] C. Bellecci, I. Bellucci, P. Gaudio, S. Martellucci, G. Petrocelli, and M. Richetta, Rev. Sci. Instrum. **74**, 1064 (2003).
[4] L. J. Dhareshwar, P. A. Naik, and D. D. Bhawalkar, Rev. Sci. Instrum. **62**, 369 (1991).
[5] J. X. Ma, D. R. Alexander, and D. E. Poulain, Combust. Flame **112**, 492 (1998).
[6] T. X. Phuoc, C. M. White, and D. H. McNeill, Opt. Lasers Eng. **38**, 217 (2002).
[7] C. G. Morgan, Rep. Prog. Phys. **38**, 621 (1975).
[8] N. Kroll and K. Watson, Phys. Rev. A **5**, 1883 (1972).
[9] I. C. E. Turcu, M. C. Gower, and P. Huntington, Opt. Commun. **134**, 66 (1997).
[10] A. Sircar, R. K. Dwivedi, and R. K. Thareja, Appl. Phys. B: Lasers Opt. **63**, 623 (1996).
[11] A. J. Alcock, K. Kato, and M. C. Richardson, Opt. Commun. **6**, 342 (1972).
[12] Y. Gamal, L. El-Nadi, M. O. Omara, B. Ghazoulin, and K. A. Sabour, J. Phys. D **32**, 1633 (1999).
[13] T. X. Phuoc, Opt. Commun. **175**, 419 (2000).
[14] D. I. Rosen and G. Weyl, J. Phys. D **20**, 1264 (1987).
[15] A. Vogel, K. Nahen, D. Theisen, R. Birngruber, R. J. Thomas, and B. A. Rockwell, Appl. Opt. **38**, 3636 (1999).
[16] L. R. Evans and C. G. Morgan, Phys. Rev. Lett. **22**, 1099 (1969).
[17] Zeemax, 10.0 ed. (Focus Software Inc., Tucson, AZ, 2001).
[18] S. S. Harilal, C. V. Bindhu, M. S. Tillack, F. Najmabadi, and A. C. Gaeris, J. Appl. Phys. **93**, 2380 (2003).
[19] J. B. Simeonsson and A. W. Miziolek, Appl. Opt. **32**, 939 (1993).
[20] S. Yalcin, D. R. Crosley, G. P. Smith, and G. W. Faris, Appl. Phys. B: Lasers Opt. **68**, 121 (1999).
[21] M. Longenecker, L. Huwel, L. Cadwell, and D. Nassif, Appl. Opt. **42**, 990 (2003).
[22] D. C. Smith, Opt. Eng. **20**, 962 (1981).
[23] V. I. Bergel'son, T. V. Loseva, I. V. Nemchinov, and T. I. Orlova, Sov. J. Plasma Phys. **1**, 498 (1975).
[24] T. A. Spiglanin, A. McIlroy, E. W. Fournier, R. B. Cohen, and J. A. Syage, Combust. Flame **102**, 310 (1995).
[25] Y. L. Chen, J. W. L. Lewis, and C. Parigger, J. Quant. Spectrosc. Radiat. Transf. **67**, 91 (2000).
[26] S. S. Harilal, C. V. Bindhu, R. C. Issac, V. P. N. Nampoori, and C. P. G. Vallabhan, J. Appl. Phys. **82**, 2140 (1997).
[27] R. K. Singh and J. Narayan, Phys. Rev. B **41**, 8843 (1990).